

# Constraints on neutrino masses from WMAP5 and BBN in the lepton asymmetric universe

Maresuke Shiraishi,<sup>1</sup> Kazuhide Ichikawa,<sup>2</sup> Kiyotomo Ichiki,<sup>1</sup> Naoshi Sugiyama,<sup>1,3</sup> and Masahide Yamaguchi<sup>4</sup>

<sup>1</sup>*Department of Physics and Astrophysics, Nagoya University, Aichi 464-8602, Japan\**

<sup>2</sup>*Department of Micro Engineering, Kyoto University, Kyoto 606-8501, Japan*

<sup>3</sup>*Institute for the Physics and Mathematics of the Universe (IPMU),*

*The University of Tokyo, Kashiwa, Chiba, 277-8568, Japan*

<sup>4</sup>*Department of Physics and Mathematics, Aoyama Gakuin University, Sagami-hara 229-8558, Japan*

(Dated: April 4, 2019)

In this paper, we put constraints on neutrino properties such as mass  $m_\nu$  and degeneracy parameters  $\xi_i$  from WMAP5 data and light element abundances by using a Markov chain Monte Carlo (MCMC) approach. In order to take consistently into account the effects of the degeneracy parameters, we run the Big Bang Nucleosynthesis code for each value of  $\xi_i$  and the other cosmological parameters to estimate the Helium abundance, which is then used to calculate CMB anisotropy spectra instead of treating it as a free parameter. We find that the constraint on  $m_\nu$  is fairly robust and does not vary very much even if the lepton asymmetry is allowed, and is given by  $\sum m_\nu < 1.3$  eV (95% C.L.).

PACS numbers: 98.80.Cq

## I. INTRODUCTION

Neutrino masses are the key feature beyond the standard model of particle physics because neutrinos are assumed to be massless in the minimal standard model. However, oscillation experiments recently suggest tiny but non-zero masses of neutrinos. Unfortunately they can probe the mass (squared) differences between different mass eigenstates but cannot determine absolute neutrino masses. The most stringent constraint on the sum of neutrino masses comes from cosmological observations. For example, by using the SDSS luminous red galaxies [1], the sum of neutrino masses is constrained as  $\sum m_\nu < 0.9$  eV (95% C.L.), though there is still uncertainty in the galaxy bias. On the other hand, Ichikawa et al.[2, 3] showed that similar constraint can be obtained by CMB data alone, which is free from such an uncertainty and the most conservative. The latest WMAP results yield  $\sum m_\nu < 1.3$  eV (95% C.L.) for the  $\Lambda$ CDM model [4]. This constraint is shown to be robust over the different cosmological models, even if we abandon the assumption of the spatial flatness of the universe, change the equation of state of dark energy, and include tensor modes [2, 3, 4, 5].

Another assumption in the standard cosmology that is usually taken is the symmetry in the lepton sector. This is closely related to cosmological neutrinos since neutrinos have all the lepton number of the universe due to its electronic charge neutrality. The standard sphaleron process forces the amount of lepton asymmetry to be the same order as that of baryon asymmetry. However, several ways are proposed to avoid such sphaleron effects [6, 7, 8, 9, 10, 11, 12, 13, 14, 15]. For example, if  $Q$ -balls are formed after the Affleck-Dine leptogenesis, the large lepton asymmetry inside  $Q$ -balls is protected from sphaleron effects and the unprotected small lepton asymmetry is converted into the small baryon asymmetry [11]. Thus, small baryon asymmetry is naturally compatible with large lepton asymmetry. In addition, observational constraint on lepton asymmetry is much weaker than that of baryon asymmetry. Then, one may wonder how robust the constraint on neutrino masses is in the possible presence of large lepton asymmetry. This is the main topic we would like to pursue in this paper.

The lepton asymmetry which is usually denoted by the degenerate parameter  $\xi$  is an interesting quantity to be constrained [16, 17, 18, 19], where  $\xi$  is defined as a chemical potential between neutrino and anti-neutrino normalized by the neutrino temperature. Recently, Popa and Vasilie have obtained a limit on  $\xi$  by using the WMAP 5 year data combined with the other CMB data and the LSS data [19]. However, since there are uncertainties of biasing and non-linearity as regards galaxy clustering data, it would be useful to constrain  $\xi$  from WMAP5 alone. We also consider indirect effects of  $\xi$  on CMB through the primordial helium abundance  $Y_p$  generated during the process of the Big Bang Nucleosynthesis (BBN).

---

\*Electronic address: mare@a.phys.nagoya-u.ac.jp

In this analysis, we consider three light neutrinos, based on the result of high energy experiments such as LEP, i.e.  $N_\nu = 2.984 \pm 0.008$  [20]. We assume equal neutrino masses between flavors, such as  $m_\nu \equiv m_{\nu_e} = m_{\nu_\mu} = m_{\nu_\tau}$ , which yields  $\sum m_\nu = 3m_\nu$ . It is because the accuracy of the present cosmological observation is not yet up to specify their mass differences. Potentially, the degeneracy parameter  $\xi$  can take different values for each flavor of neutrinos. In this paper we consider the two cases: one is the case that  $\xi_e = \xi_\mu = \xi_\tau$ , and the other is that  $\xi_\mu = \xi_\tau \equiv \xi_{\mu,\tau} \neq \xi_e$ . The first case is motivated by Refs. [21, 22, 23], which show that if a flavor mixing angle of neutrino  $\theta_{13}$  is large enough, each degeneracy parameter becomes same before BBN, namely  $\xi_e = \xi_{\mu,\tau}$ . However, as recently stressed by Ref. [24], while this conclusion is basically correct, oscillations take place so late that perfect equilibrium is never achieved and the ratio of imperfectness strongly depends on the magnitude of  $\theta_{13}$  [24]. It is also pointed out that if a Nambu-Goldstone particle such as majoron  $\eta$  interacts with neutrinos, flavor mixing can be suppressed and leads  $\xi_e \neq \xi_{\mu,\tau}$  [25]. Therefore, we also consider the second case  $\xi_e \neq \xi_{\mu,\tau}$ . The second case is also motivated by the fact that  $\xi_\mu$  and  $\xi_\tau$  have the same effects both on the BBN and CMB because we consider the degenerate masses, while  $\xi_e$  does not.

This paper is organized as follows. In the next section, we summarize effects of  $m_\nu$  and  $\xi_i$  on BBN and CMB. In Sec. III, we give the cosmological model that we use in parameter searching of MCMC analysis. In Sec. IV, we present our limits from the observational data based on WMAP5 and explain the correlation between the bound of each parameter. In final section V, we provide the summary of this paper. Throughout this paper, we set  $c = \hbar = 1$ .

## II. COSMOLOGICAL EFFECTS OF $\xi_i$ AND $m_\nu$

In this section, we review the effects of the neutrino mass  $m_\nu$  and the degeneracy parameter  $\xi_i$  on the predicted helium abundance  $Y_p$  in BBN theory and the predicted CMB power spectrum  $C_l$ . The degeneracy parameter of  $i$ th flavor of neutrino is defined as

$$\xi_i \equiv \frac{\mu_{\nu_i}}{T_\nu}, \quad (1)$$

where  $\mu_{\nu_i}$  is the chemical potential.

### A. Effects on BBN

The observed primordial light-element abundances constrain the conditions during the BBN epoch from the time of weak reaction freeze out ( $t \sim 1\text{sec}$ ,  $T \sim 1\text{MeV}$ ) to the freeze out of nuclear reactions ( $t \sim 10^4\text{sec}$ ,  $T \sim 10\text{keV}$ ). In the standard BBN theory, the abundance of light elements is determined by only one parameter, namely, baryon-to-photon ratio. However, the lepton asymmetry changes the abundance in two ways.

The one is that the extra energy density coming from the neutrino degeneracy changes the expansion rate of the universe during the BBN epoch and hence the primordial abundances. Specifically, the Fermi-Dirac distribution functions of neutrinos and anti-neutrinos with neutrino degeneracy are given by

$$f_{\nu_i}(q, \xi_i) = \frac{1}{1 + e^{q - \xi_i}}, \quad f_{\bar{\nu}_i}(q, \xi_i) = \frac{1}{1 + e^{q + \xi_i}}, \quad (2)$$

where  $q$  is comoving momentum written by proper momentum  $P$  and neutrino temperature  $T_\nu$  as  $q \equiv P/T_\nu$ , and  $\xi_i$  is the degeneracy parameter of  $i$ th flavor of neutrino. The energy density for massless degenerate neutrinos is given by

$$\rho_\nu + \rho_{\bar{\nu}} = \sum_i (k_B T_\nu)^4 \int \frac{d^3 q}{(2\pi)^3} q (f_{\nu_i}(q, \xi_i) + f_{\bar{\nu}_i}(q, \xi_i)) \equiv \frac{N_{\text{eff}}}{3} (\rho_{\nu_0} + \rho_{\bar{\nu}_0}), \quad (3)$$

where  $\rho_{\nu_0}$  is the energy density for massless non-degenerate neutrinos and  $N_{\text{eff}}$  is the effective number of relativistic degrees of freedom of neutrinos given by

$$N_{\text{eff}} \equiv \left( 1 + \frac{30}{7} \left( \frac{\xi_e}{\pi} \right)^2 + \frac{15}{7} \left( \frac{\xi_e}{\pi} \right)^4 \right) + 2 \left( 1 + \frac{30}{7} \left( \frac{\xi_{\mu,\tau}}{\pi} \right)^2 + \frac{15}{7} \left( \frac{\xi_{\mu,\tau}}{\pi} \right)^4 \right). \quad (4)$$

In the non-degenerate neutrino case,  $N_{\text{eff}} = 3$ . Therefore the neutrino degeneracy increases the energy density of neutrino.

The other is that positive  $\xi_e$  suppresses  $p \rightarrow n$  weak reactions and leads the neutron-to-proton ratio to smaller value both in and out of the chemical equilibrium. Therefore the abundance of helium  $Y_p$  decreases monotonically with

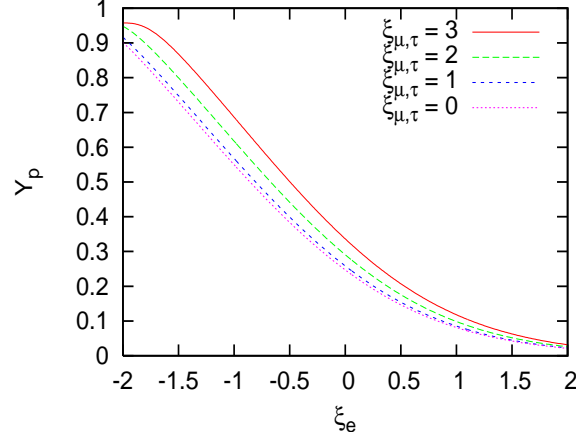


FIG. 1: Effects of the degeneracy parameters,  $\xi_e$  and  $\xi_{\mu,\tau}$ , on the helium abundance  $Y_p$ . Here we fix the baryon abundance  $\omega_b$  to the mean value from WMAP5 alone analysis for a power-law flat  $\Lambda$ CDM model [4].

increasing  $\xi_e$ . Note that the dependence on  $m_\nu$  can be neglected because  $m_\nu$  is much smaller than the temperature at the BBN epoch and does not affect the reaction rate.

We used the Kawano BBN code [26] to include the two effects described above and to calculate the abundance of light elements correctly. We also updated the nuclear reaction rates [27]. In Fig. 1, the effects of  $\xi_e$  and  $\xi_{\mu,\tau}$  on the helium abundance  $Y_p$  are demonstrated. The larger  $N_{\text{eff}}$  makes the universe expand faster and more neutrons survive before the nucleosynthesis begins. Therefore the helium abundance becomes larger as  $\xi_{\mu,\tau}$  increases. On the other hand,  $Y_p$  decreases monotonically as  $\xi_e$  increases because the chemical potential of electron type neutrinos suppresses the neutron-proton ratio at the onset of BBN as mentioned above.

### B. Effects on CMB

Cosmological Microwave Background (CMB) photons are the remnants from the Big-Bang in the early universe. They have evolved through the interaction with the matters and the gravitational potentials, and have been released from the last scattering surface at cosmological recombination ( $z \sim 1088$ ) to reach us through the large scale structure of the universe. Therefore CMB contains plenty of information about the energy contents of the universe. In the simplest cosmological model, the universe is assumed to be spatially flat, and neutrinos are massless and not degenerate. The angular power spectrum of the CMB,  $C_l$ , can be described by the six cosmological parameters, namely, the energy density of baryon and dark matter, the present Hubble parameter, the amplitude of the primordial curvature perturbation and its spectral index, and the optical depth due to re-ionization. However, if  $m_\nu$  and  $\xi_i$  are finite values, both of them also affect  $C_l$  both at the background and the perturbation levels.

In the background evolution, the mass of neutrino  $m_\nu$  and the neutrino degeneracy  $\xi_i$  determine the energy density and pressure of neutrinos. The energy density of massive degenerate neutrinos is described as  $\rho_\nu + \rho_{\bar{\nu}} = \sum_i m_\nu (n_{\nu_i}(\xi_i) + n_{\bar{\nu}_i}(\xi_i))$ , where  $n_{\nu_i}$  is the number density of neutrinos. Therefore the energy density parameter of them, which is the normalized energy density by the critical density  $\rho_{\text{crit}} = (3H^2)/(8\pi G)$ , is given as

$$\Omega_\nu = \frac{m_\nu (\Theta_2(\xi_e) + 2\Theta_2(\xi_{\mu,\tau}))}{k_B T_\nu(0)} \frac{\rho_{\nu_0}(0) + \rho_{\bar{\nu}_0}(0)}{\rho_{\text{crit}}(0)}. \quad (5)$$

Here the argument (0) means the value at present and the  $n$ th moment is defined as

$$\Theta_n(\xi_i) \equiv \frac{1}{2} \int q^n dq (f_{\nu_i} + f_{\bar{\nu}_i}) / \left( \frac{7\pi^4}{120} \right). \quad (6)$$

When we can regard neutrinos as massless degenerate particles,  $\rho_\nu + \rho_{\bar{\nu}}$  is expressed by using  $N_{\text{eff}}$  just like the discussion in the previous subsection.

Meanwhile, in the perturbation evolution, the  $\xi_i$  changes on the gravitational source term of the collisionless Boltzmann equation of neutrino. Specifically, its coefficient,  $df/dq$ , is modified as

$$\frac{d \ln(f_{\nu_i} + f_{\bar{\nu}_i})}{d \ln q} = - \frac{q}{e^{-q} + \cosh \xi_i} \frac{1 + \cosh \xi_i \cosh q}{\cosh \xi_i + \cosh q}. \quad (7)$$

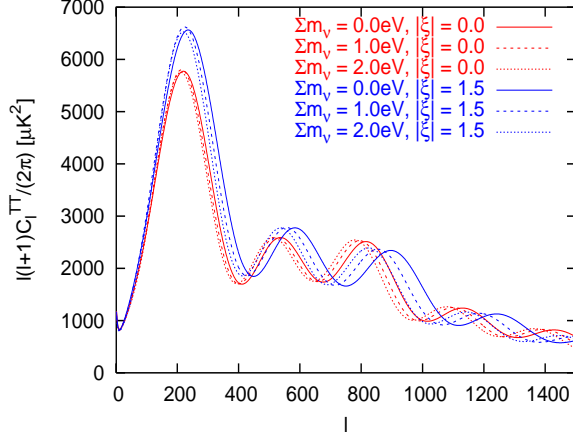


FIG. 2: Effects of  $m_\nu$  and  $\xi$  on  $C_l^{TT}$  for the case  $\xi_e = \xi_{\mu,\tau}$  with massless neutrinos. Two dotted lines and a dashed line are  $C_l^{TT}$ 's affected with  $Y_p$  fixed as 0.24. Here we fix  $\omega_b + \omega_c$  and change  $\omega_\nu$  by  $Y_p$  related with  $\xi$  at BBN. Solid lines show  $C_l^{TT}$ 's affected by Other cosmological parameters are taken as the mean value from  $Y_p$  unrelated with  $\xi$ . Here we fix  $\omega_b + \omega_c$ . Other cosmological WMAP5 alone analysis for a power-law flat  $\Lambda$ CDM model [4] i.e.  $\Omega_b + \Omega_c + \Omega_\nu + \Omega_\Lambda = 1$ .

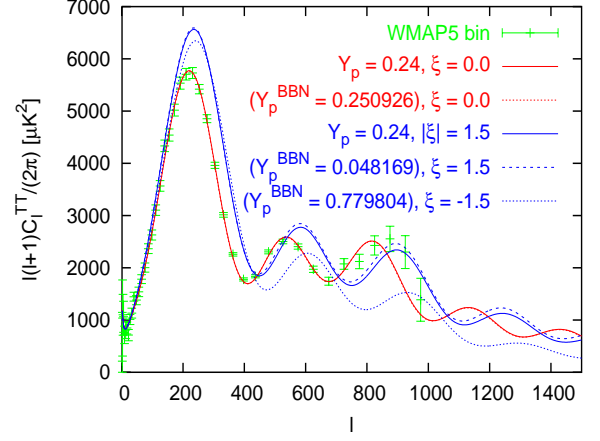


FIG. 3: Effects of  $\xi$  on  $C_l^{TT}$  for the case  $\xi_e = \xi_{\mu,\tau}$  with massless neutrinos. Two dotted lines and a dashed line are  $C_l^{TT}$ 's affected with  $Y_p$  fixed as 0.24. Here we fix  $\omega_b + \omega_c$  and change  $\omega_\nu$  by  $Y_p$  related with  $\xi$  at BBN. Solid lines show  $C_l^{TT}$ 's affected by Other cosmological parameters are taken as the mean value from  $Y_p$  unrelated with  $\xi$ . Here we fix  $\omega_b + \omega_c$ . Other cosmological WMAP5 alone analysis for a power-law flat  $\Lambda$ CDM model [4] i.e.  $\Omega_b + \Omega_c + \Omega_\nu + \Omega_\Lambda = 1$ .

Because we consider the situation that neutrinos have degenerate masses, and because neutrinos are collisionless at the CMB epoch irrelevant to their flavors, there are no difference in the effects on  $C_l$  between  $\xi_e$  and  $\xi_{\mu,\tau}$  contrary to the product  $Y_p$  at BBN. For the details of the effects of  $m_\nu$  and  $\xi$  on CMB we refer readers to the references [28, 29]. Here we derived above equations following their notations.

We inserted these two modifications in the Boltzmann Code for Anisotropies in the Microwave Background (CAMB) [30, 31, 32]. Then we checked the consistency between the  $C_l$ 's given by [29] and those calculated using our modified code. In Fig. 2, effects of  $m_\nu$  and  $\xi$  on the CMB temperature power spectrum  $C_l^{TT}$  are demonstrated.

Now we explain the dependence of  $\xi_i$  and  $m_\nu$  on the CMB spectrum. If the effective number of neutrino,  $N_{\text{eff}}$ , increases by increasing  $|\xi_i|$ , the sound horizon at the last scattering becomes smaller and the epoch of radiation-matter equality delays leading the larger decay of the gravitational potential. These effects shift  $C_l$  to the higher  $l$  and derive the enhancement of the 1st peak. In addition, through the effects of free streaming of these ultra-relativistic neutrinos, the smaller scale gravitational potentials have been damped just prior to the beginning of the acoustic oscillations of the baryon-photon fluid. This causes the smaller temperature fluctuations. These effects on  $C_l$  from  $N_{\text{eff}}$  are discussed in detail in [33].

Next we focus our attention on the dependence of  $m_\nu$  [2, 34]. In massive non-degenerate case ( $\xi_i = 0$ ), neutrino mass of  $O(\text{eV})$  causes overall horizontal shift and suppression around the first peak (when we fix  $\omega_b + \omega_c$  and change  $\omega_\nu$  to keep flatness). The horizontal shift comes from the fact that the larger  $m_\nu$  (more non-relativistic particles at present epoch) implies that the distance to the last scattering surface is shorter and the peaks move to smaller  $l$ . However, this shift is mostly canceled by the downward shift in  $H_0$ . Therefore this does not produce a neutrino mass signal. If  $m_\nu \gtrsim 0.6 \text{ eV}$ , massive neutrinos on average become non-relativistic before the epoch of recombination and only in this case, the neutrino mass can significantly imprint a characteristic signal in acoustic peaks (specifically, the matter-radiation equality occurs earlier due to less relativistic degrees of freedom and 1st peak is suppressed by the smaller early-integrated Sachs-Wolfe effect) [2, 34].

In massive degenerate case ( $\xi_i \neq 0$ ), the behavior of  $C_l$  can be understood by combining the effects in the massless degenerate case and the massive non-degenerate case. In Fig. 2 we depict the CMB angular power spectrum to illustrate the effects of mass and degeneracy of neutrinos. We see that the  $m_\nu$ -dependence does not much depend on  $\xi$ . As mentioned above, roughly speaking, neutrino mass constraint from (WMAP-level) CMB observation is determined by a critical mass  $3m_{\nu,c}$  which is defined by  $z_{\text{rec}} \simeq z_{\text{nr}}$ , where  $z_{\text{nr}}$  denotes the redshift when neutrinos on average become non-relativistic. When there is a finite  $\xi$ , the neutrino momentum distribution is modified and so is this critical mass. In this case, the critical mass is obtained by

$$\frac{m_{\nu,c}(\xi)}{m_{\nu,c}(\xi=0)} \simeq \frac{P_\nu(\xi)}{P_\nu(\xi=0)} \simeq F_\nu(\xi) \quad (8)$$

where  $P_\nu(\xi)$  and  $P_\nu(\xi=0)$  are the average momenta of neutrinos in massive degenerate and massive non-degenerate

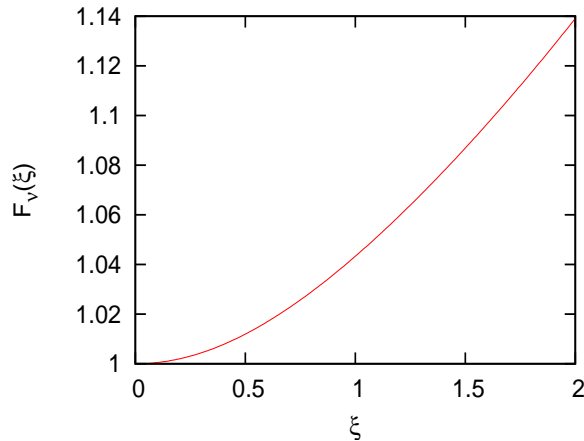


FIG. 4: The ratio of the neutrino masses between degenerate and non-degenerate cases for which the neutrinos become non-relativistic at recombination.

cases, given by  $P_\nu \approx \rho_\nu/n_\nu$ , and  $F_\nu$  is given by

$$F_\nu(\xi) \equiv \left( 1 + \frac{30}{7} \left( \frac{\xi}{\pi} \right)^2 + \frac{15}{7} \left( \frac{\xi}{\pi} \right)^4 \right) \frac{\Theta_2(\xi=0)}{\Theta_2(\xi)}. \quad (9)$$

Numerically we depict  $F_\nu$  in Fig. 4. From the figure we found  $F_\nu \lesssim 1.14$  for  $\xi < 2$ . Therefore the critical mass ( $3m_{\nu,c}(\xi=0) = 1.7$  eV for massive non-degenerate case) shifts to, at most, 1.9 eV for massive degenerate case. As it is indicated [2] that  $m_\nu$  is already limited less than  $m_{\nu,c}$ , we can expect that the upper bound of  $\sum m_\nu$  from CMB is almost invariant even in the lepton asymmetric universe, as will be shown later.

Finally, we briefly explain the dependence of the CMB power spectrum on  $Y_p$ . The main effect of  $Y_p$  on the CMB power spectrum comes from the diffusion damping at small scales. When  $Y_p$  is larger, the number of free electron becomes smaller, because the maximum number of free electron in the fully ionized universe is proportional to  $(1 - Y_p/2)$ . The number of free electron becomes even smaller at the epoch of hydrogen recombination, since it is easier for electrons to recombine with  $^4\text{He}$  than with H and consequently more electrons have been captured into the  $^4\text{He}$  nuclei by that epoch. Thus the Compton mean free path becomes larger for larger  $Y_p$ , which mean that the diffusion length of photon becomes also larger. Since the photon-baryon tight coupling breaks down at the photon diffusion scales, the fluctuation of photon is exponentially damped due to the diffusive mixing and re-scattering. Hence the CMB power spectrum is damped more for larger values of  $Y_p$ . Detailed explanations are found in Refs. [35, 36, 37]. This effect is rather small and not relevant to WMAP5 level observation. However, in our case, since  $Y_p$  can take very large or small value with  $\xi \sim O(1)$ , this may affect constraints. For example, two models with  $\xi_e = \xi_{\mu,\tau} = 1.5$  and  $-1.5$  give the same CMB spectra if we fix  $Y_p = 0.24$ . However, if we consider the effects of  $\xi$  at BBN epoch correctly, the two models predict  $Y_p = 0.048$  and  $0.780$ , respectively as shown in Fig. 1. Therefore, the model with negative degeneracy parameter should lead the larger diffusion damping as shown in Fig. 3. The CMB power spectrum can be affected by  $\xi$  through such an indirect manner [38].

### III. MODEL AND LIKELIHOOD ANALYSIS

In what follows we will put constraints on the neutrino degeneracy parameters  $\xi_i$  and masses  $m_\nu$  along with the other standard cosmological parameters. For this purpose we implement CAMB and BBN codes modified by us for lepton asymmetric cosmology in the CosmoMC Monte Carlo Markov Chain (MCMC) public package [39]. In our analysis we use observational data set in several combinations; WMAP5 alone, WMAP5 + prior on Hubble parameter ( $H_0 = 72 \pm 8$  km/sec/Mpc (68% C.L.)) given by Hubble Space Telescope (HST) [40], and WMAP5 +  $^4\text{He}$  and D/H abundances (BBN). Throughout our analysis we assume that the universe is spatially flat and neutrinos are degenerate in mass. We explore the likelihood in 10 dimensional parameter space, i.e.,

$$\vec{p} = (\omega_b, \omega_{\text{dm}}, A_s, n_s, \theta_s, \tau, A_{\text{SZ}}, \xi_e, \xi_{\mu,\tau}, \omega_\nu). \quad (10)$$

Here  $\omega_b$ ,  $\omega_{\text{dm}}$  and  $\omega_\nu$  are the energy densities of baryon, dark matter, and massive neutrino, respectively,  $A_s$  and  $n_s$  are the amplitude and the spectral index of the primordial density perturbation power spectrum at the pivot scale

$k_* = 0.002 \text{ Mpc}^{-1}$ ,  $\theta_s$  is the acoustic peak scale,  $\tau$  is the optical depth of reionization, and  $A_{\text{SZ}}$  is the amplitude parameter of thermal Sunyaev-Zel'dovich (SZ) effect [41]. Note that  $\omega_\nu$  is included in  $\omega_{dm}$  so that  $\omega_{dm} \equiv \omega_c + \omega_\nu$ , where  $\omega_c$  is the energy density of cold dark matter. As for the helium abundance  $Y_p$  used in CMB calculations, we consider two situations: the one is that we (approximately) fix  $Y_p = 0.24$  regardless of the cosmological parameters, and the other is that  $Y_p$  is derived at each time of MCMC step from the other cosmological parameters using the modified BBN code. Hereafter we denote for the latter case the helium abundance as  $Y_p^{BBN}$ , i.e.,

$$Y_p = Y_p^{BBN}(\omega_b, \xi_e, \xi_{\mu, \tau}). \quad (11)$$

Note that for the former case we vary the degeneracy parameter  $\xi$  freely in the MCMC analysis even if the helium abundance is kept fixed as  $Y_p = 0.24$ .

In the usual CMB constraints the helium abundance is often fixed to the standard value, say  $Y_p = 0.24$ . This condition is justified by the fact that current CMB measurements have already put a tight constraint on  $\omega_b$ , and for this constrained range of  $\omega_b$  the CMB spectrum does not change very much even if we allow the helium abundance to vary according to the standard BBN prediction.

However, in the lepton asymmetric universe considered in this paper, the value of  $Y_p$  can deviate significantly from  $Y_p = 0.24$  depending on  $\xi$  as discussed above. In this sense, any analysis of CMB constraint on  $\xi$  with fixed  $Y_p$  is inconsistent unless  $\xi$  is constrained tightly. In our CMB power spectrum calculation as is used in later analysis,  $Y_p$  is set by the BBN theoretical calculation as a function of  $\omega_b$ ,  $\xi_e$  and  $\xi_{\mu, \tau}$ . We also investigate constraints in the lepton asymmetric models with fixed  $Y_p$  for comparison.

#### IV. RESULTS AND COMPARISONS

In this section, we describe our results and give their interpretations. For a test calculation we first ran CosmoMC to constrain neutrino masses from WMAP5 alone with  $\xi = 0$ . We obtained consistent but slightly tighter result,  $\sum m_\nu < 1.2 \text{ eV}$  (95%CL), while WMAP team obtained 1.3 eV [5]. This difference would be attributed to differences in the treatment of cosmological parameters as well as their priors [42] [43]. In general, posterior distributions depend on prior distributions in Bayesian estimation [39].

Next, we ran a MCMC with all of the parameters to be fixed other than  $\xi_{\mu, \tau}$  and confirmed that the 1D posterior distributions of  $\xi_{\mu, \tau}$  are symmetric about  $\xi = 0$ . Using this fact we restricted the prior range of  $\xi_{\mu, \tau}$  only to positive values, i.e., we actually estimate  $|\xi_{\mu, \tau}|$  from MCMC analysis.

We perform MCMC analyses for three combinations of observational data sets described below. In all analyses, we neglect effects of CMB lensing because they slightly change  $C_l$  but do not change the posterior distributions very much.

##### A. Constraints from WMAP5 alone

We first present the result of constraints on cosmological parameters from WMAP5 alone in TABLE I. In that table, we focus on 5 parameters,  $\xi_i, m_\nu, H_0, Y_p, \omega_{dm}$ . For cosmological models we consider the following four cases and give the results separately. We present the mean values and 68% and 95% confidence regions for the case  $\xi_e = \xi_{\mu, \tau}$  in the left panel of TABLE I, and for the case  $\xi_e \neq \xi_{\mu, \tau}$  in the right panel. For each panel we separate the results for cases whether we use BBN code to calculate  $Y_p$  or we approximately fixed  $Y_p$  value to 0.24. The results for the massless neutrino cases are given in the appendix.

As is found in TABLE I, the constraints on  $\xi$  from CMB are highly dependent on whether one fixes helium abundance or derives it from BBN theory. First, let us consider the case with fixed helium abundance. In this case, the constraints on  $\xi$  from CMB becomes symmetric about  $\xi_i = 0$ , because positive and negative  $\xi$  give identical effects on the CMB spectrum through Eqs. (4) (5), and (7). In reality, however, the positive and negative  $\xi$  give different effects on the CMB spectrum through the helium abundance. In CMB theory, helium abundance is related to the number density of free electrons, and hence the Silk damping scale depends on it. So the CMB can put constraint on  $Y_p$ , and therefore  $\xi$  is further constrained through this effect if one derives helium abundance from BBN theory for the CMB calculations. From the fact that the current upper limit on helium abundance from CMB is found to be  $Y_p < 0.44$  and there is no lower bound [37], negative  $\xi_e$  is disfavored, because negative  $\xi_e$  leads to large  $Y_p$  as is discussed in II A. As for the other cosmological parameters, such as  $\omega_b$  and  $n_s$ , are tightly constrained for all cases and the constraints do not change between different models considered here, because the dependence of these parameters on  $C_l$  does not degenerate with that of  $\xi_i$  and  $Y_p$ .

One may find it inconsistent that the constraints on  $\xi_e$  and  $\xi_{\mu, \tau}$  with fixed  $Y_p = 0.24$  are different because in this case  $\xi_e$  and  $\xi_{\mu, \tau}$  play the same role in the CMB. However, in fact, the bound of  $\xi_{\mu, \tau}$  should be tighter than that of

parameter	$\xi \equiv \xi_e = \xi_{\mu,\tau}$		$\xi_e \neq \xi_{\mu,\tau}$	
	$Y_p = 0.24$	$Y_p = Y_p^{BBN}$	$Y_p = 0.24$	$Y_p = Y_p^{BBN}$
$100\omega_b$	$2.205 \pm 0.070$	$2.206^{+0.072}_{-0.074}$	$2.200^{+0.069}_{-0.070}$	$2.199 \pm 0.075$
$\omega_{dm}$	$0.1823^{+0.015}_{-0.043}$	$0.1799^{+0.0079}_{-0.0501}$	$0.2111^{+0.0202}_{-0.0477}$	$0.2158^{+0.0208}_{-0.0575}$
$\xi_e$	$< 2.41$	$1.20^{+0.50+1.39}_{-0.40-1.61}$	$< 3.47$	$1.65^{+0.63+2.00}_{-0.68-1.84}$
$ \xi_{\mu,\tau} $	-	-	$< 2.70$	$< 2.81$
$\sum m_\nu$ (eV)	$< 1.2$	$< 1.3$	$< 1.2$	$< 1.3$
$Y_p$	-	$< 0.36$	-	$< 0.32$

TABLE I: Mean values and 68% C.L. errors of the cosmological parameters obtained from the analysis of WMAP5 alone in the lepton asymmetric universe with massive neutrinos. For the constraints on  $\xi$ , 95% C.L. errors are also shown, and the upper bounds on  $\xi$ ,  $\sum m_\nu$ , and  $Y_p$  are at 95% C.L. The left side of the table is in the case of  $\xi_e = \xi_{\mu,\tau}$ . The right side is in the case  $\xi_e \neq \xi_{\mu,\tau}$ . Two parameters at the bottom are the derived parameters from the MCMC sampling.

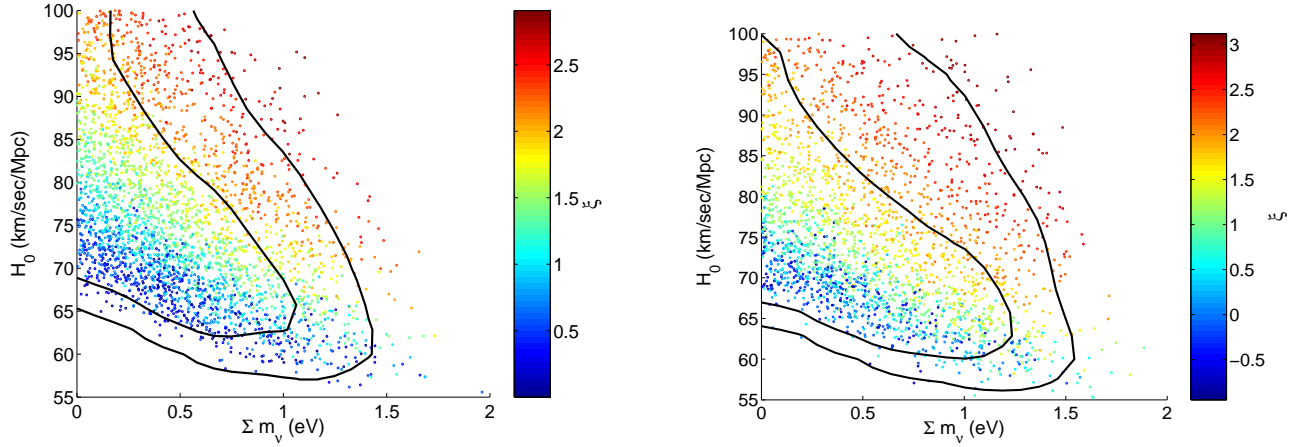


FIG. 5: The constraints in the 3D region of  $\sum m_\nu$ ,  $H_0$  and  $\xi$  from WMAP5 alone in the case of  $\xi_e = \xi_{\mu,\tau}$  with  $Y_p = 0.24$  (the left figure) or  $Y_p = Y_p^{BBN}$  (the right one). The density of the points, whose colors are coded according to the value of  $\xi$ , represent the probability distribution from MCMC samples. The contours are the 68% and 95% confidence regions.

$\xi_e$  because we implicitly assume the condition  $\xi_\mu = \xi_\tau$  in this analysis. We analytically estimated this difference as  $|\xi_e/\xi_{\mu,\tau}| \sim 1.3$ , which can be derived as follows. If we varied each of the degeneracy parameter freely, the distributions for  $\xi_e$ ,  $\xi_\mu$  and  $\xi_\tau$  should have been identical in the case where helium abundance is kept fixed and the masses are degenerated. The effects of  $\xi$  in this case mainly come through an increase of neutrino energy density, i.e., Eq. (4). Therefore, once the constraints on  $\xi_e$  can be obtained in the form as

$$\frac{30}{7} \left( \frac{\xi_e}{\pi} \right)^2 + \frac{15}{7} \left( \frac{\xi_e}{\pi} \right)^4 < \alpha, \quad (12)$$

with some value of  $\alpha$ , then, the constraints on  $\xi_{\mu,\tau}$  should read

$$2 \left[ \frac{30}{7} \left( \frac{\xi_{\mu,\tau}}{\pi} \right)^2 + \frac{15}{7} \left( \frac{\xi_{\mu,\tau}}{\pi} \right)^4 \right] < \alpha. \quad (13)$$

We found that this estimate is in good agreement with our MCMC constraints. The result of the constraints from WMAP5 alone is depicted on  $H_0$ - $\sum m_\nu$  plane in Fig. 5. In that figure, the points are drawn such that the density of the points is proportional to the number of the MCMC samples (i.e., probability distributions), and colors represent the value of  $\xi$ . One can see from this figure a well-known  $H_0$ - $\sum m_\nu$  degeneracy with fixed  $\xi$  values. We find that the upper bound of  $\sum m_\nu$  is not changed significantly because this upper bound is lower than the critical mass  $3m_{\nu,c}$ . It is interesting to note that the massive neutrino cosmology with  $\sum m_\nu \approx 1$  eV is compatible with the Hubble parameter  $H_0 \approx 72$  km/sec/Mpc if one allows  $\xi \approx 1$  lepton asymmetry, as will be discussed in the next subsection.

From WMAP5 alone, the upper bounds of  $\xi_i$  are actually determined by the flat prior on the  $H_0$  which is taken as

parameter	$\xi \equiv \xi_e = \xi_{\mu,\tau}$	$\xi_e \neq \xi_{\mu,\tau}$
$100\omega_b$	$2.202^{+0.069}_{-0.072}$	$2.193^{+0.072}_{-0.073}$
$\omega_{dm}$	$0.1621^{+0.0045}_{-0.0384}$	$0.1947^{+0.0132}_{-0.0451}$
$\xi_e$	$0.96^{+0.50+1.35}_{-0.40-1.52}$	$1.48^{+0.55+1.92}_{-0.64-1.68}$
$ \xi_{\mu,\tau} $	-	$< 2.50$
$\sum m_\nu$ (eV)	$< 1.3$	$< 1.4$
$Y_p$	$< 0.41$	$< 0.32$
$H_0$ (km/sec/Mpc)	$71.8^{+2.2}_{-3.0}$	$74.0^{+2.8}_{-3.4}$

TABLE II: Mean values and 68% C.L. errors of the cosmological parameters obtained from the analysis of WMAP5 + HST in the lepton asymmetric universe with massive neutrinos. For the constraints on  $\xi$ , 95% C.L. errors are also shown, and the upper bounds on  $\xi$ ,  $\sum m_\nu$ , and  $Y_p$  are at 95% C.L. The left side of the table is in the case of  $\xi_e = \xi_{\mu,\tau}$ . The right side is in the case of  $\xi_e \neq \xi_{\mu,\tau}$ . Here we use the relation  $Y_p = Y_p^{BBN}$  in the calculation of the CMB power spectra. Three parameters at the bottom are the derived parameters from the MCMC sampling.

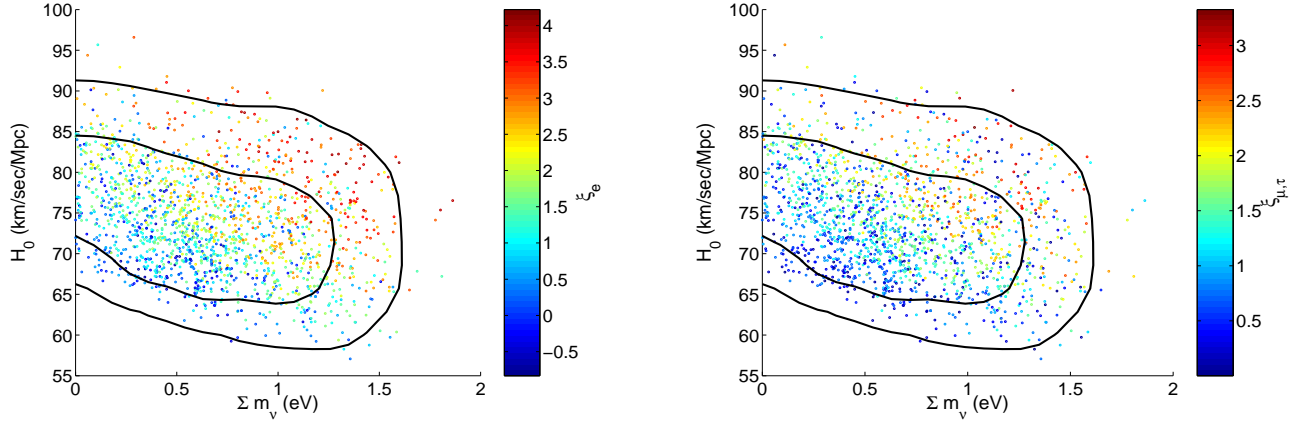


FIG. 6: The constraint in the 3D region of  $\sum m_\nu$ ,  $H_0$  and  $\xi_e$  (the left figure) or  $\xi_{\mu,\tau}$  (the right one) from WMAP5 + HST in the massive  $\xi_e \neq \xi_{\mu,\tau}$  case with  $Y_p = Y_p^{BBN}$ . The points and contours are depicted in the same way as Fig. 5.

$H_0 < 100$  km/sec/Mpc. Therefore, analysis which takes into account external prior on  $H_0$  should be performed. In the next subsection, we apply a prior of  $H_0$  from HST.

### B. Constraints from WMAP5 + HST

In this subsection, we present the constraints from WMAP5 + HST, with the helium abundance being set to  $Y_p^{BBN}$  (see Eq. (11)). Here the prior from HST is  $H_0 = 72 \pm 8$  km/sec/Mpc (68% C.L.) [40]. These results are presented in TABLE II.

In TABLE II, we found that all the parameters except for  $\sum m_\nu$  and  $Y_p$  are limited more tightly than those limited from WMAP5 alone. This is due to breaking the  $H_0 - \xi$  degeneracy.

In the standard non-degenerate case, by adding HST prior the upper bound of  $\sum m_\nu$  becomes tighter than that from WMAP5 alone, and we found  $\sum m_\nu < 1.0$  eV. This is because the prior of HST breaks effectively the well-known  $\sum m_\nu - H_0$  degeneracy. Interestingly, however, we found that the upper bounds of  $\sum m_\nu$  from WMAP5 + HST do not change very much compared with the upper bounds from WMAP5 alone if the lepton asymmetry is allowed. In the degenerate case, higher neutrino masses are compatible with the Hubble parameter around  $H_0 \approx 72$  km/sec/Mpc with non-zero  $\xi$ , as depicted in Fig. 6. This is because the shift of the peak to the lower  $l$  due to larger  $m_\nu$  can be compensated by the shift due to larger  $\xi$ , with the Hubble parameter fixed. Therefore, HST prior does not improve the limits on neutrino masses in the lepton asymmetric universe.



parameter	$\xi \equiv \xi_e = \xi_{\mu,\tau}$	$\xi_e \neq \xi_{\mu,\tau}$
$100\omega_b$	$2.215 \pm 0.066$	$2.221 \pm 0.061$
$\omega_{dm}$	$0.1147^{+0.0079}_{-0.0078}$	$0.1311^{+0.0056}_{-0.0096}$
$\xi_e$	$-0.013^{+0.016}_{-0.017} \pm 0.033$	$0.034^{+0.017+0.075}_{-0.025-0.058}$
$ \xi_{\mu,\tau} $	-	$< 1.60$
$\sum m_\nu$ (eV)	$< 1.2$	$< 1.1$
$Y_p$	$0.250 \pm 0.004$	$0.250 \pm 0.004$
$H_0$ (km/sec/Mpc)	$66.4^{+4.4}_{-4.6}$	$70.0^{+2.7}_{-3.1}$

TABLE III: Mean values and 68% C.L. errors of the cosmological parameters obtained from the analysis of WMAP5 + BBN in the lepton asymmetric universe with massive neutrinos. For the constraints on  $\xi$ , 95% C.L. errors are also shown, and the upper bounds on  $\xi$  and  $\sum m_\nu$  are at 95% C.L.. The left side of the table is in the case of  $\xi_e = \xi_{\mu,\tau}$ . The right side is in the case of  $\xi_e \neq \xi_{\mu,\tau}$ . Here we use the relation  $Y_p = Y_p^{BBN}$  in the calculation of the CMB power spectra. Three parameters at the bottom are the derived parameters from the MCMC sampling.

### C. Constraints from WMAP5 + BBN

Finally, we present the constraints from WMAP5 combined with observations of light element abundances of  $Y_p$  and  $D/H$ . We use only  $Y_p = 0.250 \pm 0.004$  [44] in the case  $\xi_e = \xi_{\mu,\tau}$ . In the case  $\xi_e \neq \xi_{\mu,\tau}$ , there is a parameter degeneracy between  $\xi_e$  and  $\xi_{\mu,\tau}$  for the constraint from the helium abundance alone. Therefore, we further use the deuterium abundance constraint as  $D/H = (2.82 \pm 0.27) \times 10^{-5}$  [45] in this case to break the degeneracy. The results are listed in TABLE. III, and our constraints on the sum of neutrino masses are 1.2 eV and 1.1 eV respectively for the cases  $\xi_e = \xi_{\mu,\tau}$  and  $\xi_e \neq \xi_{\mu,\tau}$ . They do not depend on the assumption of  $\xi_e = \xi_{\mu,\tau}$  and  $\xi_e \neq \xi_{\mu,\tau}$ . Again, we have found that neutrino mass constraints do not change much depending on the assumptions on  $\xi$ .

As for the constraints on the degeneracy parameters, we obtain  $\xi = -0.013^{+0.016}_{-0.017}$  in the case  $\xi_e = \xi_{\mu,\tau}$ , and  $\xi_e = 0.034^{+0.017}_{-0.025}$  and  $|\xi_{\mu,\tau}| < 1.60$  in the case  $\xi_e \neq \xi_{\mu,\tau}$  from WMAP5 + BBN. In relation to them, we also performed a conventional analysis. Namely, we searched three-dimensional parameter space of  $\omega_b$ ,  $\xi_e$  and  $\xi_{\mu,\tau}$  by BBN calculation. Here, we take the baryon density of  $\omega_b = 0.0225 \pm 0.0006$  obtained from WMAP5 data in flat  $\Lambda$ CDM model. The constraints,  $\xi = -0.013^{+0.016}_{-0.017}$  in the case  $\xi_e = \xi_{\mu,\tau}$ , and  $\xi_e = 0.002^{+0.056}_{-0.024}$  and  $|\xi_{\mu,\tau}| < 1.61$  in the case  $\xi_e \neq \xi_{\mu,\tau}$  are consistent with the cases above confirming the validity of the conventional procedure.

## V. SUMMARY

In this paper, we have discussed the effects of neutrino masses and neutrino degeneracies on CMB and BBN, and investigated how the latest observations put constraints on these properties simultaneously. In particular, we have examined how robust the constraint on neutrino masses is in the lepton asymmetric universe. Our constraints on the neutrino masses are  $m_\nu < 1.3$  eV at 95% C.L. from WMAP alone. The constraint does not change very much even if we put the HST prior in the lepton asymmetric universe, as explained in Sec.IVB. We investigate the two types of lepton asymmetry, i.e. the cases with  $\xi_e = \xi_{\mu,\tau}$  and  $\xi_e \neq \xi_{\mu,\tau}$ , and found that the constraints are almost the same for both cases. We also have taken into account the measurements of light element abundances, and found that changes in constraints are very small. These results are summarized in Fig. 7.

As for constraints on the degeneracy parameters, we have obtained at 95% C.L.  $-0.41 < \xi_e < 2.59$  for  $\xi_e = \xi_{\mu,\tau}$ . In the case of  $\xi_e \neq \xi_{\mu,\tau}$ , the constraints are  $-0.19 < \xi_e < 3.65$  and  $|\xi_{\mu,\tau}| < 2.81$  from WMAP5 alone. We point out that they are limits obtained by imposing the BBN relation for  $Y_p$  and this helps to place tight lower bound on  $\xi_e$ . Although these constraints are much weaker than those obtained from  $Y_p$  measurements in HII regions and direct use of BBN theory, this would be more useful in future CMB measurements such as Planck [19, 38] to constrain  $\xi_e$ .

### Acknowledgments

This work is supported in part by the Grant-in-Aid for Scientific Research from the Ministry of Education, Science, Sports, and Culture of Japan No. 21740177 (K.I.) and No. 21740187 (M.Y.). This work is supported in part by the Grant-in-Aid for Scientific Research on Priority Areas No. 467 "Probing the Dark Energy through an Extremely Wide and Deep Survey with Subaru Telescope" and by the Grant-in-Aid for Nagoya University Global COE Program,

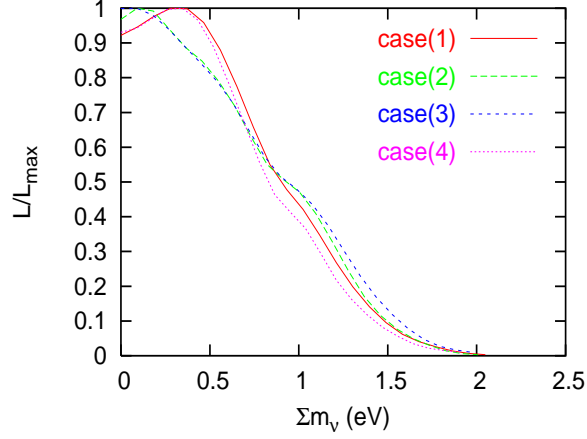


FIG. 7: One dimensional posterior distribution of  $\sum m_\nu$  in the specific 4 cases. Case (1): the WMAP5 alone constraint with  $Y_p = 0.24$  and no lepton asymmetry, Case (2): the WMAP5 alone constraint with  $Y_p = Y_p^{BBN}$  and  $\xi_e = \xi_{\mu,\tau}$ , Case (3): WMAP5 alone constraint with  $Y_p = Y_p^{BBN}$  and  $\xi_e \neq \xi_{\mu,\tau}$ , Case (4): the WMAP5+BBN constraint with  $Y_p = Y_p^{BBN}$  and  $\xi_e \neq \xi_{\mu,\tau}$ .

"Quest for Fundamental Principles in the Universe: from Particles to the Solar System and the Cosmos", from the Ministry of Education, Culture, Sports, Science and Technology of Japan.

#### APPENDIX A: CONSTRAINTS FOR THE MASSLESS DEGENERATE CASE

In this Appendix, we present the result of constraints on cosmological parameters for massless degenerate case with  $Y_p$ 's relation as  $Y_p = Y_p^{BBN}$ . In TABLE IV and V, we show all the results. In this case, basically, the bounds are determined by the similar effects as we discussed in the massive case. Here we stress the point simplified by dealing with neutrinos as massless particles is that  $H_0$  is completely determined by the degeneracy effect of  $H_0 - N_{\text{eff}}$  reported in [33] once  $\xi$ 's is limited by the effect of  $Y_p$ .

parameter	WMAP5 alone	WMAP5 + HST	WMAP5 + BBN
$100\omega_b$	$2.258 \pm 0.063$	$2.251^{+0.063}_{-0.062}$	$2.250^{+0.063}_{-0.062}$
$\omega_{dm}$	$0.1421^{+0.0079}_{-0.0254}$	$0.1220^{+0.0031}_{-0.0106}$	$0.1080 \pm 0.0062$
$\xi$	$0.91^{+0.54+1.21}_{-0.41-1.50}$	$0.42^{+0.39+1.05}_{-0.36-1.13}$	$-0.013 \pm 0.017^{+0.034}_{-0.032}$
$N_{\text{eff}}$	$< 10.2$	$< 6.18$	$< 3.002$
$Y_p$	$< 0.42$	$< 0.45$	$0.250 \pm 0.004$
$H_0$ (km/sec/Mpc)	-	$75.3^{+1.3}_{-2.6}$	$71.9 \pm 2.7$

TABLE IV: Mean values and 68% C.L. errors of the cosmological parameters obtained from the analysis of WMAP5 alone, WMAP5 + HST, and WMAP5 + BBN in the lepton asymmetric universe with massless neutrinos. For the constraints on  $\xi$ , 95% C.L. errors are also shown, and the upper bounds on  $N_{\text{eff}}$ , and  $Y_p$  are at 95% C.L. Here we consider the case  $\xi_e = \xi_{\mu,\tau}$  and use the relation  $Y_p = Y_p^{BBN}$ . Three parameters at the bottom are the derived parameters from the MCMC sampling.

- 
- [1] M. Tegmark, D. J. Eisenstein, M. A. Strauss, D. H. Weinberg, M. R. Blanton, J. A. Frieman, M. Fukugita, J. E. Gunn, A. J. S. Hamilton, G. R. Knapp, et al., Phys. Rev. D **74**, 123507 (2006), arXiv:astro-ph/0608632.
  - [2] K. Ichikawa, M. Fukugita, and M. Kawasaki, Phys. Rev. D **71**, 043001 (2005), arXiv:astro-ph/0409768.
  - [3] M. Fukugita, K. Ichikawa, M. Kawasaki, and O. Lahav, Phys. Rev. D **74**, 027302 (2006), arXiv:astro-ph/0605362.
  - [4] E. Komatsu, J. Dunkley, M. R. Nolta, C. L. Bennett, B. Gold, G. Hinshaw, N. Jarosik, D. Larson, M. Limon, L. Page, et al., ApJS **180**, 330 (2009), 0803.0547.
  - [5] J. Dunkley, E. Komatsu, M. R. Nolta, D. N. Spergel, D. Larson, G. Hinshaw, L. Page, C. L. Bennett, B. Gold, N. Jarosik, et al., ApJS **180**, 306 (2009), 0803.0586.

parameter	WMAP5 alone	WMAP5 + HST	WMAP5 + BBN
$100\omega_b$	$2.257^{+0.062}_{-0.063}$	$2.249^{+0.062}_{-0.061}$	$2.253 \pm 0.059$
$\omega_{dm}$	$0.1614^{+0.0133}_{-0.0256}$	$0.1343^{+0.0063}_{-0.0139}$	$0.1256^{+0.0059}_{-0.0097}$
$\xi_e$	$1.22^{+0.58+1.74}_{-0.64-1.61}$	$0.74^{+0.43+1.46}_{-0.52-1.26}$	$0.040^{+0.047+0.093}_{-0.045-0.070}$
$ \xi_{\mu,\tau} $	$< 2.35$	$< 1.78$	$< 1.67$
$N_{\text{eff}}$	$< 10.7$	$< 7.13$	$< 5.78$
$Y_p$	$< 0.38$	$< 0.41$	$0.250 \pm 0.004$
$H_0$ (km/sec/Mpc)	-	$77.8^{+2.1}_{-2.9}$	$76.4^{+1.9}_{-2.7}$

TABLE V: The same as TABLE IV, but for the case with  $\xi_e \neq \xi_{\mu,\tau}$ .

- [6] K. Enqvist, K. Kainulainen, and J. Maalampi, Nuclear Physics B **349**, 754 (1991).
- [7] R. Foot, M. J. Thomson, and R. R. Volkas, Phys. Rev. D **53**, 5349 (1996), arXiv:hep-ph/9509327.
- [8] X. Shi, Phys. Rev. D **54**, 2753 (1996), arXiv:astro-ph/9602135.
- [9] A. Casas, W. Y. Cheng, and G. Gelmini, Nuclear Physics B **538**, 297 (1999), arXiv:hep-ph/9709289.
- [10] J. McDonald, Physical Review Letters **84**, 4798 (2000), arXiv:hep-ph/9908300.
- [11] M. Kawasaki, F. Takahashi, and M. Yamaguchi, Phys. Rev. D **66**, 043516 (2002), arXiv:hep-ph/0205101.
- [12] M. Yamaguchi, Phys. Rev. D **68**, 063507 (2003), arXiv:hep-ph/0211163.
- [13] T. Chiba, F. Takahashi, and M. Yamaguchi, Physical Review Letters **92**, 011301 (2004), arXiv:hep-ph/0304102.
- [14] F. Takahashi and M. Yamaguchi, Phys. Rev. D **69**, 083506 (2004), arXiv:hep-ph/0308173.
- [15] M. Laine and M. Shaposhnikov, Journal of Cosmology and Astro-Particle Physics **6**, 31 (2008), 0804.4543.
- [16] A. D. Dolgov, Phys. Rep. **370**, 333 (2002), arXiv:hep-ph/0202122.
- [17] P. D. Serpico and G. G. Raffelt, Phys. Rev. D **71**, 127301 (2005), arXiv:astro-ph/0506162.
- [18] V. Simha and G. Steigman, Journal of Cosmology and Astro-Particle Physics **8**, 11 (2008), 0806.0179.
- [19] L. A. Popa and A. Vasilie, Journal of Cosmology and Astro-Particle Physics **6**, 28 (2008), 0804.2971.
- [20] J. Dress, ed., *The LEP Collaborations and the LEP Electroweak Working Group @ the XX International Symposium on Lepton and Photon Interactions at High Energy, Rome, Italy* (2001).
- [21] A. D. Dolgov, S. H. Hansen, S. Pastor, S. T. Petcov, G. G. Raffelt, and D. V. Semikoz, Nuclear Physics B **632**, 363 (2002), arXiv:hep-ph/0201287.
- [22] Y. Y. Wong, Phys. Rev. D **66**, 025015 (2002), arXiv:hep-ph/0203180.
- [23] K. N. Abazajian, J. F. Beacom, and N. F. Bell, Phys. Rev. D **66**, 013008 (2002), arXiv:astro-ph/0203442.
- [24] S. Pastor, T. Pinto, and G. Raffelt, ArXiv e-prints (2008), 0808.3137.
- [25] A. D. Dolgov and F. Takahashi, Nuclear Physics B **688**, 189 (2004), arXiv:hep-ph/0402066.
- [26] L. Kawano, preprint FERMILAB-Pub-92/04-A (1992).
- [27] C. Angulo, M. Arnould, M. Rayet, P. Descouvemont, D. Baye, C. Leclercq-Willain, A. Coc, S. Barhoumi, P. Aguer, C. Rolfs, et al., Nuclear Physics A **656**, 3 (1999).
- [28] K. Ichiki, M. Yamaguchi, and J. Yokoyama, Phys. Rev. D **75**, 084017 (2007), arXiv:hep-ph/0611121.
- [29] J. Lesgourgues and S. Pastor, Phys. Rev. D **60**, 103521 (1999), arXiv:hep-ph/9904411.
- [30] A. Cooray, W. Hu, and M. Tegmark, ApJ **540**, 1 (2000), arXiv:astro-ph/0002238.
- [31] A. Challinor and A. Lewis, Phys. Rev. D **71**, 103010 (2005), arXiv:astro-ph/0502425.
- [32] A. Lewis, A. Challinor, and A. Lasenby, ApJ **538**, 473 (2000), arXiv:astro-ph/9911177.
- [33] K. Ichikawa, T. Sekiguchi, and T. Takahashi, Phys. Rev. D **78**, 083526 (2008), 0803.0889.
- [34] K. Ichikawa, Journal of Physics Conference Series **120**, 022004 (2008), 0711.2622.
- [35] R. Trotta and S. H. Hansen, Phys. Rev. D **69**, 023509 (2004), arXiv:astro-ph/0306588.
- [36] K. Ichikawa and T. Takahashi, Phys. Rev. D **73**, 063528 (2006), arXiv:astro-ph/0601099.
- [37] K. Ichikawa, T. Sekiguchi, and T. Takahashi, Phys. Rev. D **78**, 043509 (2008), 0712.4327.
- [38] J. Hamann, J. Lesgourgues, and G. Mangano, Journal of Cosmology and Astro-Particle Physics **3**, 4 (2008), 0712.2826.
- [39] A. Lewis and S. Bridle, Phys. Rev. D **66**, 103511 (2002), arXiv:astro-ph/0205436.
- [40] W. L. Freedman, B. F. Madore, B. K. Gibson, L. Ferrarese, D. D. Kelson, S. Sakai, J. R. Mould, R. C. Kennicutt, Jr., H. C. Ford, J. A. Graham, et al., ApJ **553**, 47 (2001), arXiv:astro-ph/0012376.
- [41] E. Komatsu and U. Seljak, MNRAS **336**, 1256 (2002), arXiv:astro-ph/0205468.
- [42] K. Ichiki, M. Takada, and T. Takahashi, Phys. Rev. D **79**, 023520 (2009), 0810.4921.
- [43] *Eiichiro Komatsu gave the indication in the private communication* (2009).
- [44] M. Fukugita and M. Kawasaki, ApJ **646**, 691 (2006), arXiv:astro-ph/0603334.
- [45] J. M. O'Meara, S. Burles, J. X. Prochaska, G. E. Prochter, R. A. Bernstein, and K. M. Burgess, ApJ **649**, L61 (2006), arXiv:astro-ph/0608302.